Graph Fourier Transform to mitigate the effects of crosstalk in hdEEG recordings

Andrea Ranieri[1,2], Jlenia Toppi[1,2]
[1] *Department of Computer, Control, and Management Engineering, Sapienza University of Rome, Rome, Italy*
[2] *Neuroelectrical Imaging and BCI Laboratory, Fondazione Santa Lucia Hospital, Rome, Italy*

email: andrea.ranieri@uniroma1.it, jlenia.toppi@uniroma1.it

***Abstract*—Electroencephalography (EEG) is probably the most popular non-invasive technique for the acquisition of brain signals. Despite its ease of use and moderate costs, this technique intrinsically suffers from poor spatial resolution, which is known to be caused by the combinations of the volume conduction effect and crosstalk phenomena. While the first one is caused by the propagation of a source signal through different biological tissues, the second one relates to the positioning of the electrodes on the scalp, manifesting as a spurious electric signal involving a set of neighboring electrodes even in absence of true brain activity. The presence of such a spurious signal not only contributes to the spatial blurring of EEG-based scalp maps, but is also known to alter brain connectivity estimate. In this work, the simultaneous engagement of adjacent electrodes typical of crosstalk was used to characterize this phenomenon in terms of network harmonics with respect to the graph structure describing the positioning of the electrodes on the scalp. In this perspective, a tailored graph filter could be used to mitigate the effects of crosstalk and improve the accuracy of multivariate brain connectivity maps. As to do so, this work investigates the effects of different graph filtering procedures on two different datasets: a set of EEG-like data recorded on a polystyrene mannequin (representing a null-case scenario for causal connectivity) and a real EEG dataset recorded from a healthy subject during the execution of simple hand movements.**

Keywords—EEG, GSP, functional connectivity

I. Introduction

Network theory and its applications are nowadays essential tools characterizing the cutting-edge of different scientific fields. The ubiquity of graph-structured data across various disciplines encouraged the development of innovative strategies with the aim to bridge the gap between signal processing and graph-structured data [1]. In the last few years Graph Signal Processing (GSP) rapidly emerged as a pioneering branch of information theory providing tailored solutions to problems involving data defined on irregular domains [2]. From a signal processing perspective, GSP successfully contributed to an important step forward in different fields, from telecommunications to modern biomedicine [1], [3].

In the field of brain imaging, for instance, it is a well-established practice to investigate the relationship between brain signals in a multivariate set (such as those originating from functional magnetic resonance images and electroencephalography) to infer a graph structure that captures specific features of the input dataset [3], [4]. However, despite the excellent resolution in time, ease of use and moderate costs that made electroencephalography (EEG) one of the most popular techniques for the acquisition of brain signals, the poor spatial resolution characterizing EEG-based scalp maps still represents a huge drawback for this neuroimaging technique. In fact, the electric activity of different brain sources cannot be accurately separated on the scalp due to the combination of the well-known volume conduction effect with crosstalk phenomena.

More in detail, the effects of volume conduction manifest when an electric potential is recorded at a certain distance from its generator and a conductive medium fills the space between the source and the receiver [5]. As for the specific case of an EEG recording, the medium includes biological tissues (e.g. the cerebrospinal fluid, skull and scalp) which both conduct and scatter the electric activity of a given neural source, causing the signal to spread over the scalp instead of being circumscribed to a restricted area above the neural source. On the other hand, crosstalk phenomena are intimately related to both the number and the positioning of the electrodes on the scalp. In considering the human scalp as a conductive layer, it is reasonable to assume that the electric activity recorded by a specific electrode is not circumscribed to the area underneath the electrode itself, but interferes with the electric activity of its neighbors [6]. This phenomenon, known as "crosstalk", is often misinterpreted as a causal influence among nearly positioned electrodes that exists even in absence of a true underlying brain activity [7]. High-density EEG setups (from 64 to 256 electrodes) are, in general, more prone to be corrupted by crosstalk, since the distance between adjacent electrodes is reduced given the presence of a high number of sensors placed on the scalp. The simultaneous engagement of adjacent electrodes implicitly describes a smooth spatial variability that could be used to characterize crosstalk phenomena from a GSP perspective.

Specifically, given the spatial dependence characterizing crosstalk phenomena, modern GSP techniques can be used to describe electrodes' crosstalk in terms of network harmonics and design tailored graph filters that mitigates undesired contribution in the original signal. In line with this, this work proposes a GSP-based approach to investigate the contribution of different network harmonics on two different datasets: a set of EEG-like data recorded from a mannequin and a set of true EEG signals extracted from a healthy subject involved in the execution of simple hand movements. As to mimic both the conductivity of the human skin and the effects of crosstalk, EEG-like signals were acquired by placing a wet towel between the head of the mannequin and the EEG cap, allowing to consider the EEG-like time series as a null-case scenario for functional connectivity analysis (since they do not reflect the presence of a true underlying brain activity while being corrupted by crosstalk). The Graph Fourier Transform (GFT) spectrum of the EEG-like data will then be

used to identify network harmonics that largely contribute to mannequin's EEG (which are expected to characterize the effects of crosstalk) and design a tailored graph filter to mitigate their contribution. The effects of such a filtering procedure will be finally investigated on a real EEG dataset by means of multivariate connectivity estimate.

II. Materials and Methods

A. Graph signal processing principles

Given an undirected graph $G(N,E)$ with vertex set N and edge set E, a graph signal is a mapping $\boldsymbol{x}$: $N \rightarrow R$ that assigns a real value to each vertex [1], [8]. A graph signal can thus be represented as a vector $\boldsymbol{x} \in R^N$ in which each entry $x(n), n = 1,\dots N$ stores the value of the signal at the n^{th} vertex of the network. The GFT of a graph signal is then defined as its projection onto the eigenbasis of the Laplacian matrix associated with $G(N,E)$ [9]. More in detail, given the eigen-decomposition of the Laplacian matrix $L = V\Lambda V^{-1}$, the GFT for the graph signal $\boldsymbol{x}$ writes

$$GFT(\boldsymbol{x}) = \boldsymbol{y} = V^{-1}\boldsymbol{x} \tag{1}$$

where $\boldsymbol{y} \in R^N$ stores the GFT coefficients for the graph signal $\mathbf{x}$, $V \in R^{N\times N}$ is the orthogonal matrix whose columns are the eigenvectors of L, the superscript $^{-1}$ denotes the inverse matrix and $\Lambda \in R^{N\times N}$ is a diagonal matrix whose entries are the eigenvalues of L.

Similarly to the Fourier Transform for signals in time domain, an ideal graph filter $F(\Lambda) \in R^{N\times N}$ is a diagonal matrix whose entries are either 0 or 1 depending on the GFT coefficients to discard or preserve [8]. This allows to rewrite the GFT coefficients of the graph signal $\boldsymbol{x}$ as

$$\boldsymbol{y} = \underbrace{F(\Lambda)\boldsymbol{y}}_{\tilde{\boldsymbol{y}}} + \underbrace{(I - F(\Lambda))\boldsymbol{y}}_{\hat{\boldsymbol{y}}} \tag{2}$$

where $\tilde{\boldsymbol{y}} \in R^N$ contains the GFT coefficients that $F(\Lambda)$ leaves unaltered, $\hat{\boldsymbol{y}} \in R^N$ collects the GFT coefficients corresponding to the suppressed network harmonics and $I \in R^{N\times N}$ is the identity matrix of order N. The graph filtered version of the original signal can then be recovered by applying the inverse transformation that projected $\boldsymbol{x}$ onto the eigenbasis of the Laplacian matrix to the filtered set of GFT coefficients

$$\tilde{\boldsymbol{x}} = V(F(\Lambda)\boldsymbol{y}) = V(F(\Lambda)(V^{-1}\boldsymbol{x})) \tag{3}$$

In this perspective, the ideal filter $F(\Lambda)$ could be designed ad hoc to suppress undesired network harmonics in the graph signal $\boldsymbol{x}$.

B. Distance-based Laplacian matrix

The relative distance between each pair of electrodes was used to extract a graph representation for the EEG acquisition cap. Specifically, being N be the number of electrodes placed on the scalp, a diffusion kernel was used to modulate the normalized Euclidean distance between each pair of electrodes. This procedure allowed to construct a full square symmetric matrix of order N whose $(i,j)^{th}$ element approaches 1 if the electrode i is close to the electrode j (and vice versa) and vanishes to 0 as their distance increases. The corresponding binary adjacency matrix $\mathcal{A} \in R^{N\times N}$ was obtained maintaining the 25% of the strongest links and the normalized Laplacian matrix was then extracted using the Spectral And Random walK (SPARK) toolbox for (di)graphs [10] as

$$L_{norm} = I - D^{-\frac{1}{2}}\mathcal{A}D^{-\frac{1}{2}} \tag{4}$$

where $I \in R^{N\times N}$ is the order N identity matrix and $D \in R^{N\times N}$ is a diagonal matrix whose entries correspond to the degree of each node (i.e. the degree matrix associated with $\mathcal{A}$).

C. Crosstalk as a slow-varying graph signal

Since crosstalk affects groups of adjacent electrodes, its contribution could be modelled as a (spurious) common mode signal involving a subset of nearly positioned electrodes. The simultaneous involvement of adjacent electrodes implicitly describes a signal with similar values on adjacent nodes or, in other words, a smooth spatial variability with respect to the underlying domain. In GSP, the spatial variability of a graph signal is captured by its total variation, which measures the smoothness of a given signal with respect to the underlying network structure [1], [9] .

In this perspective, it is reasonable to model crosstalk phenomena as a linear combination of network harmonics with a small total variation which, in other words, represent graph signals that vary slowly with respect to the underlying graph. A properly designed graph filter could then be used to mitigate the contribution of crosstalk on real EEG data by attenuating the expression of slow-varying network harmonics in the original signal.

D. Energy-based graph filter design

Since mannequin's EEG only reflects the contribution of electrodes' crosstalk and given that crosstalk is supposed to be properly modelled as a linear combination of slow-varying network harmonics, it is reasonable to hypothesize for the energy of the mannequin's GFT spectrum to be largely expressed with a few slow-varying harmonics. In this perspective, a properly designed graph filter could be used to mitigate the contribution of undesired network harmonics, which are expected to be largely expressed in the GFT spectrum of the EEG-like signals.

As to do so, we split the total energy of the mannequin's GFT spectrum in two according to the median-split criterion before the application of an ideal high-pass graph filter that suppresses the contribution of the lower part of the spectrum [3]. The ideal graph filter is thus designed to have cutoff frequency equal to the median network harmonic $\bar{n}$ and elements on the main diagonal equal to

$$diag(F_H(\Lambda)) = \begin{cases} 1, n > \bar{n} \\ 0, n \leq \bar{n} \end{cases} \tag{5}$$

Then, the low- and high-pass graph-filtered versions of the mannequin's EEG can be respectively extracted as

$$\begin{cases} X_L = V[(I - F_H)(V^{-1}X)] \\ X_H = V[F_H(V^{-1}X)] \end{cases} \tag{6}$$

where F_H is the ideal high-pass graph filter with cut-off frequency $\bar{n}$. Both the low- (X_L) and high-pass (X_H) filtered versions of the original signal will then be used to investigate how the application of the graph filter described in Eq.5 affects the presence of crosstalk-induced spurious links in causal connectivity estimate.

E. EEG-like signal acquisition

EEG-like signals were recorded using a 30-electrode cap placed on the head of a polystyrene mannequin. Specifically, data were acquired for 2 minutes at a sampling frequency of 250 Hz using a BrainAmp amplifier (Brain Products GmbH, Germany). Reference and ground electrodes were placed on left and right mastoid respectively and the impedances were kept below 5 $k\Omega$ during the whole recording session.

In order to mimic the conductivity of the human skin, a wet towel was placed between the head of the mannequin and the EEG cap as shown in Fig.1. Lastly, data were z-scored before the extraction of multivariate functional connectivity.

F. EEG data from real scenario

Both the EEG amplifier and electrode cap introduced in Section E were then used to record a set of real EEG data from a right-handed healthy subject (female, 37 y.o.) involved in the execution of simple hand tasks. The participant signed an informed consent and experiments took place at the Neuroelectrical Imaging and Brain Computer Interface Laboratory at Fondazione Santa Lucia IRCCS in Rome, Italy, where the study was approved by the local ethics board (CE PROG.752/2019).

The experimental session consisted of four runs during which the participant sat in a comfortable chair while visual cues were presented on a screen in front of her. Each run comprises 20 task (8s duration) and 20 rest (4s duration) trials presented in a pseudo-random order. During task runs, the subject was asked to perform a simple finger extension movement with either the right or left hand (respectively indicated as ExtR and ExtL). Task trials began with a 4s-preparatory period, after which a go stimulus occurs, and the participant was asked to perform the required task for the remaining part of the trial. Instead, in rest trials the participant was asked to stay relaxed for the whole duration of the trial. During the inter-trial interval, a fixation cross was displayed for 3s in the middle of the screen

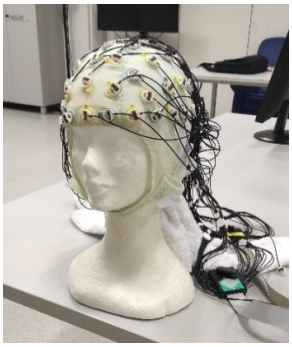

Fig.1. Positioning of the electrode cap on the mannequin. A wet towel was placed between the head of the mannequin and the EEG cap to mimic the conductivity of the human skin.

G. EEG data preprocessing and functional connectivity estimation

Both EEG-like and real brain signals were band-pass filtered within $[3-60]$ Hz and the power-line interference was removed using a 50 Hz notch filter. For real EEG data only, an Independent Component Analysis (ICA) was carried out to remove ocular artifacts and a semiautomatic procedure based on a fixed threshold criterion (± 80 μV) was then used to reject residual artifacts (e.g., muscular, environmental). Both the EEGs were finally segmented into1s lasting trials for further causal connectivity estimation.

The graph filter introduced in Section D was then used to extract the low- and high-pass graph filtered version of both the EEG-like and real brain signals. Specifically, each trial was considered as a sequence of graph signals $X \in R^{N \times T}$, where N is the number of nodes in the underlying network (i.e. the number of electrodes on the scalp) and T the number of samples in each trial. Then, the low- and high-pass filtered version of each graph signal were extracted as in Eq.6.

Functional connectivity matrices were then extracted from the filtered versions of both the EEG-like and real brain signals by means of Partial Directed Coherence (PDC), a spectral estimator relying on the multivariate autoregressive (MVAR) model of the EEG time series [11]. PDC values were averaged within four frequency bands, namely theta ($[3,7]$ Hz), alpha ($[8,12]$ Hz), beta ($[13,30]$ Hz) and gamma ($[31,40]Hz$) band, and tested against the chance level by applying the asymptotic method in [12]. For real EEG data, a non-parametric test was used to extract relevant task-versus-rest patterns. Specifically, the 95th percentile was extracted from the weights' distribution of each rest matrix and used to contrast the corresponding task matrix.

III. Results

A. Cutoff frequency for the graph filter

As shown in Fig.2, experimental findings pointed out that half of the energy contained in the mannequin's GFT spectrum is expressed by the first $\bar{n} = 3$ coefficients. This means that it is possible to write a truncated Fourier series that preserves half of the energy of the original signal using the $\bar{n} = 3$ slowest harmonics. Since the residual 50% of the energy is expressed by the remaining $N - \bar{n} = 28$ GFT coefficients, it is possible to conclude that the power spectral density (i.e. the amount of energy per network harmonics) is higher in the left part of the spectrum than in the right-one.

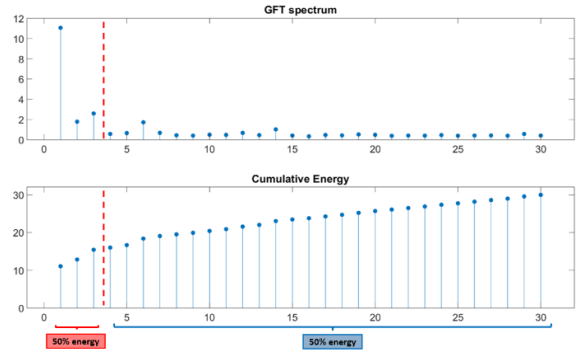

Fig.2 Energy spectrum (upper panel) and cumulative energy (lower panel) of the GFT coefficients extracted from mannequin's EEG data

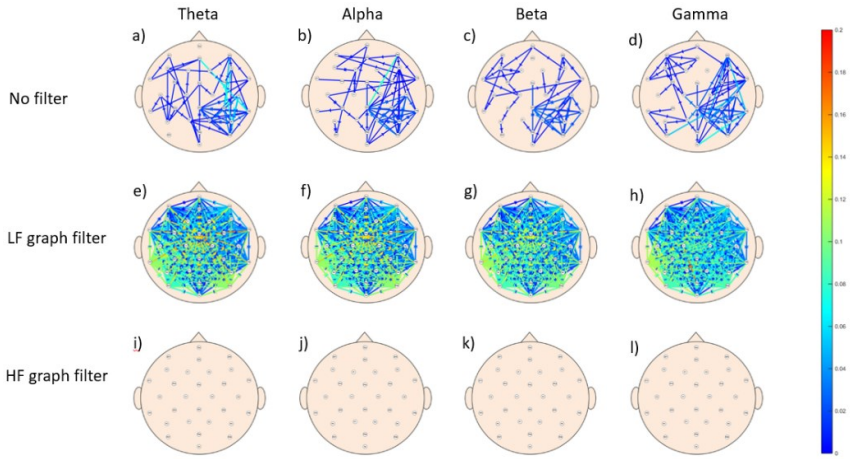

Fig.3 Functional connectivity maps extracted from mannequin's EEG-like signals without graph filtering (upper row), before the application of a low-pass graph filter (middle row) and before the application of a high-pass graph filter (last row).

B. Connectivity estimate on mannequin EEG

Results from functional connectivity estimate are shown in Fig.3 where PDC scalp maps are arranged row-wise according to the type of graph-filter applied on the EEG-like time series. Specifically: panels a), b), c) and d) show PDC scalp maps obtained without the application of any graph filtering procedure, panels e), f), g) and h) refer to scalp maps obtained applying a low-pass graph filter and panels i), j), k) and l) refer to the high-pass graph filtered version of the data. Different columns correspond to different frequency bands: the first column refers to theta, the second one to alpha, the third one to beta and the last one to gamma band respectively.

As for PDC maps extracted from the unfiltered EEG-like time series, it is possible to appreciate the presence of spurious connectivity flows characterizing the whole scalp in all the investigated frequency bands. Furthermore, the extracted connectivity patterns are not full since some of the links are associated with weights smaller than the corresponding statistical threshold. Conversely, connectivity maps extracted from the low-pass version of the EEG-like signals describe a full connectivity pattern involving all the electrodes on the scalp. The estimated PDC values have, in general, small amplitudes but are always larger than the corresponding statistical threshold. Finally, connectivity maps extracted from the high-pass EEG-like signal are empty, meaning that the estimated PDC values lie below their statistical threshold.

C. Connectivity estimate on real EEG data

Functional connectivity maps extracted from the analysis of real EEG data are shown in Fig.4. Specifically, each row shows the PDC maps extracted after the application of a different graph filter on the original EEG data, while frequency bands are arranged column-wise.

By focusing on the effects of a low-pass graph filtering procedure (first and third rows of Fig.4), it is possible to appreciate the presence of an unclear connectivity pattern characterizing the whole scalp in most of the investigated frequency bands. Regardless of the executed motor task, in fact, the extracted connectivity patterns do not exhibit a clear topological localization on the scalp. On the other hand, PDC patterns extracted after the application of a high-pass graph filter (second and fourth rows of Fig.4) exhibit a pronounced contralateralization in most of the investigated frequency bands. More in detail, it is possible to appreciate that most of the links point toward the left hemisphere during right-hand extension tasks, while direction is reversed during left-hand tasks.

IV. Discussion

When compared to the real EEG scenario, the effects of a graph filtering procedure on the EEG-like signals clearly describe the presence of a different underlying activity. Specifically, PDC maps extracted using the low-pass version of the EEG-like time series describe a dense pattern that spreads all over the scalp, regardless for the frequency band taken into account. Such a dense pattern is supposed to reflect the contribution of electrodes crosstalk since, in absence of a true brain activity, this is the only contribution that affects mannequin's EEG. In line with this, it is worth to note that all the PDC values obtained using the high-pass version of the signal are below their statistical threshold, properly reflecting the absence of a true causal relationship among the recorded set of signals. It could also be appreciated that, in line with scientific literature, the spurious connectivity flows characterizing the unfiltered version of the EEG-like time series confirms that PDC is highly sensitive to the positioning of the electrodes on the scalp [7], [13].

On the other hand, PDC maps extracted from real EEG data suffer less from the contribution of short-range links, suggesting that the effects of crosstalk are here less expressed because of the presence of a stronger underlying causal activity. In contrast to the mannequin scenario, it is interesting to appreciate that PDC maps extracted using the low-pass filtered version of the real EEG time series describe different causal patterns depending on the investigated frequency band. Such a behaviour may be related to the mixed contribution of electrodes' crosstalk and volume conduction, since the latter one is known to affect real EEG data only because of the presence of an inner source within the scalp. Furthermore, the application of a properly designed graph filter on real EEG data allowed for the extraction of causal connectivity patterns in line with the physiological principles describing the changes in brain activity during the execution of simple hand

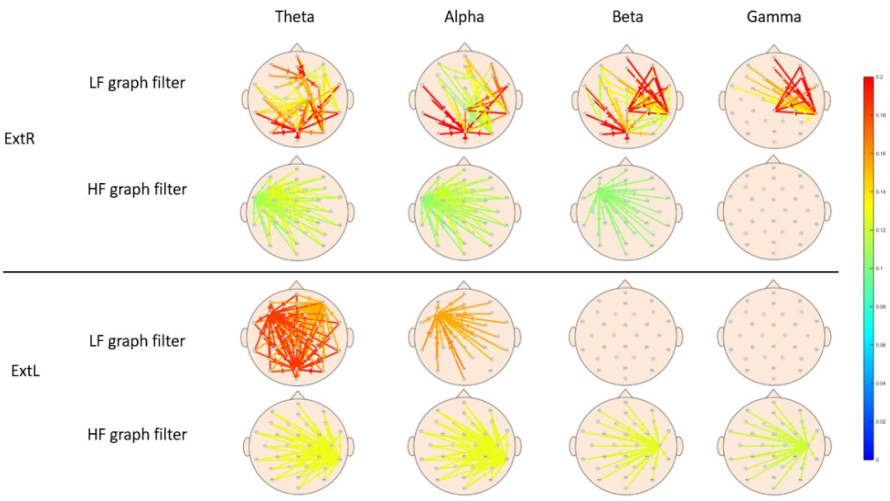

Fig.4 Functional connectivity maps extracted from a healthy subject during the execution of a finger extension task with the right (top two rows) and left (last two rows) hand.

movements. [14]. In fact, PDC maps extracted after the application of a high-pass graph filter exhibit well-defined topological properties, reflecting a pronounced contralateralization which is known to characterize the execution of simple hand movements.

V. Conclusion

This work explored the issue to characterize the contribution of different network harmonics in brain connectivity estimate. Concerning the analysis of EEG-like time series, experimental findings allowed to point out the contribution of a properly designed graph filter as a tool for mitigating the effects of crosstalk when dealing with connectivity estimate. Similarly, the application of the proposed filtering techniques to real EEG data allowed to mitigate the effects of crosstalk, promoting the extraction of connectivity patterns in line with the physiological principles governing the execution of simple hand movements in healthy subjects.

Future works should compare the proposed approach with currently used spatial filtering techniques for the EEG signal, such as the well-known surface Laplacian. Furthermore, it would also be interesting to characterize how the choice of hyperparameters (such as the number of the links used to extract the adjacency matrix) affects the filtering effect for the proposed approach.

Acknowledgment

Research supported by Sapienza University of Rome (Progetti di Avvio alla Ricerca - AR1241906EB3F9C4).

References

[1] D. I. Shuman, S. K. Narang, P. Frossard, A. Ortega, e P. Vandergheynst, «The emerging field of signal processing on graphs: Extending high-dimensional data analysis to networks and other irregular domains», *IEEE Signal Process. Mag.*, vol. 30, fasc. 3, pp. 83–98, mag. 2013, doi: 10.1109/MSP.2012.2235192.

[2] L. Stankovic, D. Mandic, M. Dakovic, M. Brajovic, B. Scalzo, e T. Constantinides, «Graph Signal Processing -- Part I: Graphs, Graph Spectra, and Spectral Clustering», 2019, *arXiv*. doi: 10.48550/ARXIV.1907.03467.

[3] M. G. Preti e D. Van De Ville, «Decoupling of brain function from structure reveals regional behavioral specialization in humans», *Nat. Commun.*, vol. 10, fasc. 1, p. 4747, ott. 2019, doi: 10.1038/s41467-019-12765-7.

[4] A. Ranieri *et al.*, «Spectral graph theory to investigate topological and dynamic properties of EEG-based brain networks: an application to post-stroke patients», in *2024 46th Annual International Conference of the IEEE Engineering in Medicine and Biology Society (EMBC)*, Orlando, FL, USA: IEEE, lug. 2024, pp. 1–4. doi: 10.1109/EMBC53108.2024.10781512.

[5] S. P. Van Den Broek, F. Reinders, M. Donderwinkel, e M. J. Peters, «Volume conduction effects in EEG and MEG», *Electroencephalogr. Clin. Neurophysiol.*, vol. 106, fasc. 6, pp. 522–534, giu. 1998, doi: 10.1016/S0013-4694(97)00147-8.

[6] F. Chella, V. Pizzella, F. Zappasodi, e L. Marzetti, «Impact of the reference choice on scalp EEG connectivity estimation», *J. Neural Eng.*, vol. 13, fasc. 3, p. 036016, giu. 2016, doi: 10.1088/1741-2560/13/3/036016.

[7] S. Haufe, V. V. Nikulin, K.-R. Müller, e G. Nolte, «A critical assessment of connectivity measures for EEG data: A simulation study», *NeuroImage*, vol. 64, pp. 120–133, gen. 2013, doi: 10.1016/j.neuroimage.2012.09.036.

[8] A. Sandryhaila e J. M. F. Moura, «Discrete Signal Processing on Graphs», *IEEE Trans. Signal Process.*, vol. 61, fasc. 7, pp. 1644–1656, apr. 2013, doi: 10.1109/TSP.2013.2238935.

[9] L. Stankovic, D. Mandic, M. Dakovic, M. Brajovic, B. Scalzo, e A. G. Constantinides, «Graph Signal Processing -- Part II: Processing and Analyzing Signals on Graphs», 2019, *arXiv*. doi: 10.48550/ARXIV.1909.10325.

[10] A. Ranieri, F. Pichiorri, E. Colamarino, F. Cincotti, D. Mattia, e J. Toppi, «SPectral graph theory And Random walK (SPARK) toolbox for static and dynamic characterization of (di)graphs: A tutorial», *PLOS One*, vol. 20, fasc. 6, p. e0319031, giu. 2025, doi: 10.1371/journal.pone.0319031.

[11] L. A. Baccalá e K. Sameshima, «Partial directed coherence: a new concept in neural structure determination», *Biol. Cybern.*, vol. 84, fasc. 6, pp. 463–474, mag. 2001, doi: 10.1007/PL00007990.

[12] «Testing the Significance of Connectivity Networks: Comparison of Different Assessing Procedures», *IEEE Trans. Biomed. Eng.*, vol. 63, fasc. 12, pp. 2461–2473, dic. 2016, doi: 10.1109/TBME.2016.2621668.

[13] J. Toppi *et al.*, «How the Statistical Validation of Functional Connectivity Patterns Can Prevent Erroneous Definition of Small-World Properties of a Brain Connectivity Network», *Comput. Math. Methods Med.*, vol. 2012, pp. 1–13, 2012, doi: 10.1155/2012/130985.

[14] G. Pfurtscheller e A. Aranibar, «Evaluation of event-related desynchronization (ERD) preceding and following voluntary self-paced movement», *Electroencephalogr. Clin. Neurophysiol.*, vol. 46, fasc. 2, pp. 138–146, feb. 1979, doi: 10.1016/0013-4694(79)90063-4.